

Notes on modeling for Kerr black holes: Basis learning, QNM frequencies, and spherical-spheroidal mixing coefficients

L. London¹

¹*School of Physics and Astronomy, Cardiff University, The Parade, Cardiff, CF24 3AA, United Kingdom*
(Dated: June 16, 2018)

The ongoing direct detection of gravitational wave signals is aided by representative models of theoretical predictions. In particular, the process of model based detection, and subsequent comparison of signals the general relativity's predictions are aided by the modeling of information related to perturbed Kerr black holes. Here, we summarize recent methods and models for the analytically understood gravitational wave spectra (quasi-normal mode frequencies), and harmonic structure of Kerr black holes (mixing coefficients between spherical and spheroidal harmonics). Towards the construction of these models, two algorithms, GMVP and GMVR, for the automated polynomial and rational modeling of general dimensional complex scalars are presented.

I. INTRODUCTION

In the coming years, expectations for frequent Gravitational wave (GW) detections of increasing signal-to-noise ratio (SNR) are high. Concurrent with Virgo, the Advanced LIGO (aLIGO) detectors will enter their third observing run in **late 2018**. At this time, binary black hole (BH) detections are expected at a rate of **X** per month. In this context, signal detection and subsequent inference of physical parameters hinges upon efficient models for source properties and dynamics. Most prominently, there is ongoing interest in signal models for binary BH inspiral, merger and ringdown (IMR). As the merger of isolated BHs is expected to result in a perturbed Kerr BH, there is related interest in having computationally efficient models for perturbative parameters, namely those that enable evaluation of the related ringdown radiation.

In particular, a perturbed Kerr BH (e.g. resulting from binary BH merger) will have GW radiation that rings down with characteristic frequencies, $\tilde{\omega}_{\ell mn} = \omega_{\ell mn} + i/\tau_{\ell mn}$. These discrete frequencies have associated radial and spatial functions which are *spheroidal* harmonic in nature. These frequencies and harmonic functions are the so-called Quasi-Normal Modes (QNMs). They are the eigen-solutions of the source free linearized Einstein's equations (i.e. Teukolsky's equations) for a perturbed BH with final mass, M_f , and dimensionless final spin, j_f . The well known and effective completeness of these solutions allows gravitational radiation from generic perturbations to be well approximated by a spectral (multipolar) sum which combines the complex QNM amplitude, $A_{\ell mn}$, with the spin weight -2 spheroidal harmonics, $_{-2}S_{\ell mn}$.

$$\begin{aligned} h &= h_+ - i h_\times \\ &= \frac{1}{r} \sum_{\ell mn} A_{\ell mn} e^{i\tilde{\omega}_{\ell mn} t} {}_{-2}S_{\ell mn}(j_f \tilde{\omega}_{\ell mn}, \theta, \phi) \\ &= \frac{1}{r} \sum_{\tilde{\ell} \tilde{m}} h_{\tilde{\ell} \tilde{m}}(t) {}_{-2}Y_{\tilde{\ell} \tilde{m}}(\theta, \phi). \end{aligned} \quad (1)$$

In the first and second lines of Eqn. (1), we relate the observable GW polarizations, h_+ and h_\times , with the analytically understood morphology of the time domain waveform. Here, the labels ℓ and m are eigenvalues of Teukolsky's angular equations, where units of $M = 1$ (e.g. the initial mass of the binary BH system), and $c = 1$. In the third line of Eqn. (1), we represent h in terms of *spherical* harmonic multipoles. This latter form is ubiquitous for the development and implementation of IMR signal models for binary BHs.

Towards the development of these models, Eqn. (1) enters in many incarnations. In the Effective One Body (EOB) formalism, $h_{\tilde{\ell} \tilde{m}}$ is modeled such that, after its peak (near merger), the effective functional form reduces (asymptotically) to Eqn. (1)'s second line. This view currently comes with the added assumption that $_{-2}S_{\ell mn} = {}_{-2}Y_{\ell m}$, where only $n = 0$ is explicitly considered. The consequences of this choice are discussed in reference [X]. For the so-called *Phenom* models, the frequency domain multipoles, $\tilde{h}_{\tilde{\ell} \tilde{m}}(f)$, are constructed such that their high frequency behavior is consistent with Eqn. (1) in the time domain.

Both Phenom and EOB approaches directly use phenomenological models (i.e. fits) for the QNM frequencies, as these fits are more computationally efficient than the underlying analytic calculations, which involve the solving of continued fraction equations. In the case of PhenomHM and derivative models, fits for the QNM frequencies are used in the process of mapping $\tilde{h}_{22}(f)$ into other $\tilde{h}_{\tilde{\ell} \tilde{m}}(f)$ [X]. In that setting, the QNM frequencies impact the morphology of each $h_{\tilde{\ell} \tilde{m}}$ in not only ringdown, but also merger and late inspiral.

For models that assist tests of the No-Hair Theorem, and thereby only include precise ringdowns, the perspective of Eqn. (1)'s second and third lines are used to write each spherical harmonic multipole moment as

$$h_{\tilde{\ell} \tilde{m}} = \frac{1}{r} \sum_{\ell mn} A_{\ell mn} e^{i\tilde{\omega}_{\ell mn} t} \sigma_{\tilde{\ell} \tilde{m} \ell mn} \quad (2)$$

where, the spherical-spheroidal mixing coefficient, $\sigma_{\tilde{\ell} \tilde{m} \ell mn}$, is

$$\sigma_{\tilde{\ell} \tilde{m} \ell mn} = \int_{\Omega} {}_{-2}S_{\ell mn} {}_{-2}Y_{\tilde{\ell} \tilde{m}}^* d\Omega. \quad (3)$$

In Eqn. (3), $*$ denotes complex conjugation, and Ω is the standard solid angle in spherical polar coordinates.

In practice, Eqn. (2) is computationally preferable: The calculation of each $_{-2}S_{\ell mn}$ involves a series solution which slowly converges for j_f near unity. Therefore, it is more effective to have accurate models for $\sigma_{\tilde{\ell} \tilde{m} \ell mn}$, which can then be used directly to calculate $h_{\tilde{\ell} \tilde{m}}$ via Eqn. (2), and thereby the GW polarizations via Eqn. (1).

In this combined context, it is clear that the modeling of QNM frequencies, $\tilde{\omega}_{\ell mn}$, and spherical-spheroidal mixing coefficients, $\sigma_{\tilde{\ell} \tilde{m} \ell mn}$, underpin a wide range of GW signal models. While models for $\tilde{\omega}_{\ell mn}$ and $\sigma_{\tilde{\ell} \tilde{m} \ell mn}$ are present in many publications, there exist minor shortcomings which we wish to address here.

For the QNM frequencies, it is well known that for nearly

$$\sigma_{22220} = 0.99733 e^{6.2813i} + 0.0075336 \frac{14.592 e^{5.0601i} \kappa + (28.761 e^{1.629i}) \kappa^2 + (14.511 e^{4.6362i}) \kappa^3 + (1.9624 e^{3.0113i})}{1 + 0.88674 e^{3.0787i} \kappa + (1.002 e^{0.13211i}) \kappa^2 + (0.082148 e^{5.6369i}) \kappa^3} \quad (13)$$

$$\sigma_{21210} = 0.99716 e^{6.2815i} + 0.0063542 \frac{1.4345 \times 10^5 e^{4.5061i} \kappa + (3.5469 \times 10^5 e^{1.7327i}) \kappa^2 + (2.4038 \times 10^5 e^{5.1629i}) \kappa^3 + (6026.9 e^{1.8881i})}{1 + 73780 e^{4.5545i} \kappa + (97494 e^{1.398i}) \kappa^2 + (34815 e^{4.5623i}) \kappa^3} \quad (14)$$

$$\sigma_{22221} = 0.99683 e^{6.2782i} + 0.020758 \frac{15.077 e^{4.8323i} \kappa + (31.139 e^{1.585i}) \kappa^2 + (15.449 e^{4.6727i}) \kappa^3 + (0.71897 e^{2.8084i})}{1 + 0.80592 e^{3.3995i} \kappa + (0.69502 e^{0.54275i}) \kappa^2 + (0.35613 e^{5.9545i}) \kappa^3} \quad (15)$$

$$\sigma_{32320} = 0.99009 e^{6.2804i} + 0.02369 \frac{71893 e^{1.2395i} \kappa + (1.7055 \times 10^5 e^{5.0371i}) \kappa^2 + (1.2947 \times 10^5 e^{2.359i}) \kappa^3 + (1935.5 e^{4.668i})}{1 + 38206 e^{1.2254i} \kappa + (35811 e^{3.9618i}) \kappa^2 + (8378.3 e^{0.11726i}) \kappa^3} \quad (16)$$

$$\sigma_{33331} = 0.99478 e^{6.2688i} + 0.040478 \frac{4.4113 e^{1.2501i} \kappa + (11.588 e^{0.27959i}) \kappa^2 + (17.322 e^{3.7904i}) \kappa^3 + (0.67724 e^{2.5797i})}{1 + 3.8782 e^{2.2864i} \kappa + (3.4913 e^{5.6655i}) \kappa^2 + (1.0368 e^{2.9082i}) \kappa^3} \quad (17)$$

$$\sigma_{32221} = 0.02203 e^{0.16452i} + 0.073233 \frac{24.932 e^{1.0181i} \kappa + (30.197 e^{4.4047i}) \kappa^2 + (11.274 e^{2.981i}) \kappa^3 + (2.4374 e^{6.1959i})}{1 + 11.397 e^{3.9953i} \kappa + (10.915 e^{5.8025i}) \kappa^2 + (7.2196 e^{1.8176i}) \kappa^3} \quad (18)$$

$$\sigma_{33330} = 0.99569 e^{6.2785i} + 0.014546 \frac{7.2112 e^{0.62811i} \kappa + (6.5381 e^{4.6216i}) \kappa^2 + (4.451 e^{2.9228i}) \kappa^3 + (1.7113 e^{2.9527i})}{1 + 1.4974 e^{1.6687i} \kappa + (1.5288 e^{5.3885i}) \kappa^2 + (0.52114 e^{2.5471i}) \kappa^3} \quad (19)$$

$$\sigma_{32220} = 0.020598 e^{0.04743i} + 0.06919 \frac{2.7657 e^{2.133i} \kappa + (3.9562 e^{4.653i}) \kappa^2 + (2.3364 e^{2.6444i}) \kappa^3 + (2.399 e^{6.2767i})}{1 + 1.0595 e^{4.7865i} \kappa + (0.91308 e^{2.887i}) \kappa^2 + (0.69468 e^{0.1912i}) \kappa^3} \quad (20)$$

$$\sigma_{43330} = 0.028112 e^{0.048488i} + 0.086383 \frac{12.087 e^{0.47221i} \kappa + (30.626 e^{3.3281i}) \kappa^2 + (16.328 e^{6.1785i}) \kappa^3 + (2.3603 e^{6.2662i})}{1 + 4.9638 e^{3.5931i} \kappa + (6.2552 e^{6.2001i}) \kappa^2 + (1.4538 e^{2.5539i}) \kappa^3} \quad (21)$$

$$\sigma_{43430} = 0.98735 e^{6.2795i} + 0.033028 \frac{7.0084 \times 10^5 e^{1.1067i} \kappa + (1.843 \times 10^6 e^{4.8808i}) \kappa^2 + (1.4367 \times 10^6 e^{2.1412i}) \kappa^3 + (13844 e^{4.5601i})}{1 + 3.5667 \times 10^5 e^{1.0149i} \kappa + (3.274 \times 10^5 e^{3.7746i}) \kappa^2 + (88621 e^{0.10095i}) \kappa^3} \quad (22)$$

$$\sigma_{44440} = 0.99478 e^{6.2776i} + 0.024791 \frac{6.5172 e^{0.79835i} \kappa + (7.7748 e^{4.2485i}) \kappa^2 + (1.1577 e^{1.5905i}) \kappa^3 + (1.2434 e^{2.9616i})}{1 + 0.44548 e^{1.2496i} \kappa + (0.59437 e^{5.6732i}) \kappa^2 + (0.24743 e^{2.8292i}) \kappa^3} \quad (23)$$

$$\sigma_{55550} = 0.99434 e^{6.2773i} + 0.03126 \frac{6.5508 e^{0.93398i} \kappa + (8.0558 e^{4.2881i}) \kappa^2 + (0.92971 e^{1.0436i}) \kappa^3 + (1.0904 e^{2.9712i})}{1 + 0.23128 e^{1.7666i} \kappa + (0.54958 e^{5.9178i}) \kappa^2 + (0.213 e^{3.0092i}) \kappa^3} \quad (24)$$

IV. DISCUSSION

-
- [1] E. Leaver, "An Analytic representation for the quasi normal modes of Kerr black holes," *Proc.Roy.Soc.Lond.*, vol. A402, pp. 285–298, 1985.

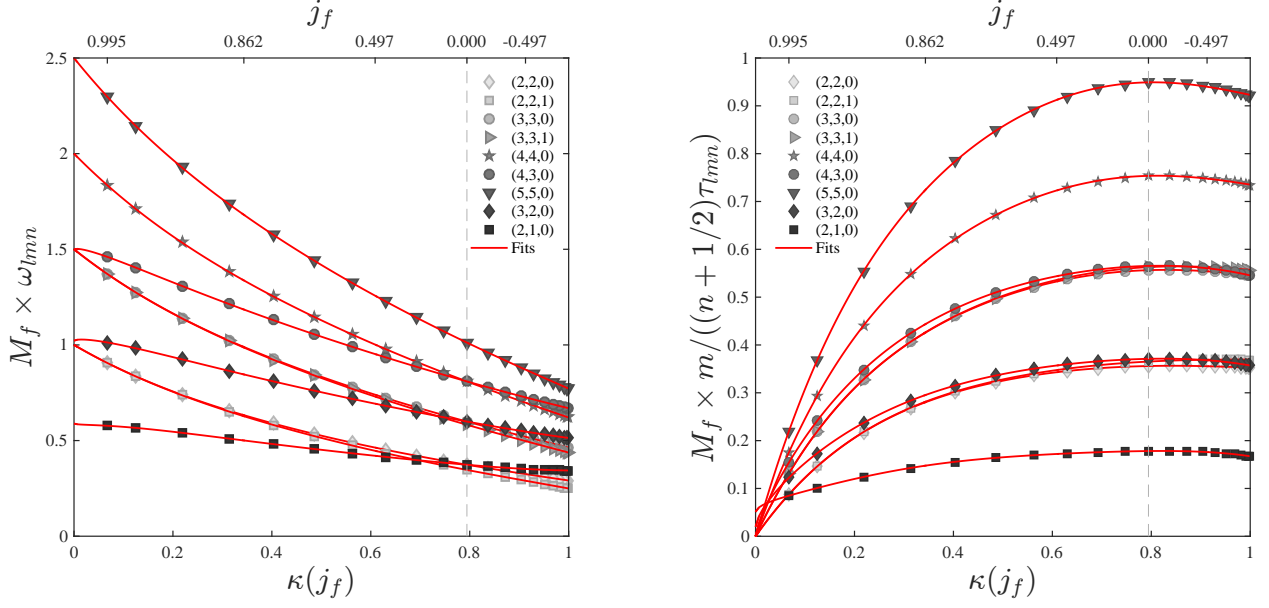


FIG. 1. Fits of dimensionless QNM central frequencies (solid lines) along with select numerical values (grey markers) computed using Leaver's method [1]. Before the application of $\kappa(j)$, points are spaced between -0.995 and 0.995 according to 0.995 times the sin of a fiducial angle which is uniformly spaced between $-\pi/2$ and $\pi/2$. Values of j are shown in the upper axis for κ at $l = m$. The grey dashed line marks the value of κ where $j = 0$. Fits of dimensionless QNM decay rates (solid lines) along with select numerical values (grey markers) computed using Leaver's method [1].

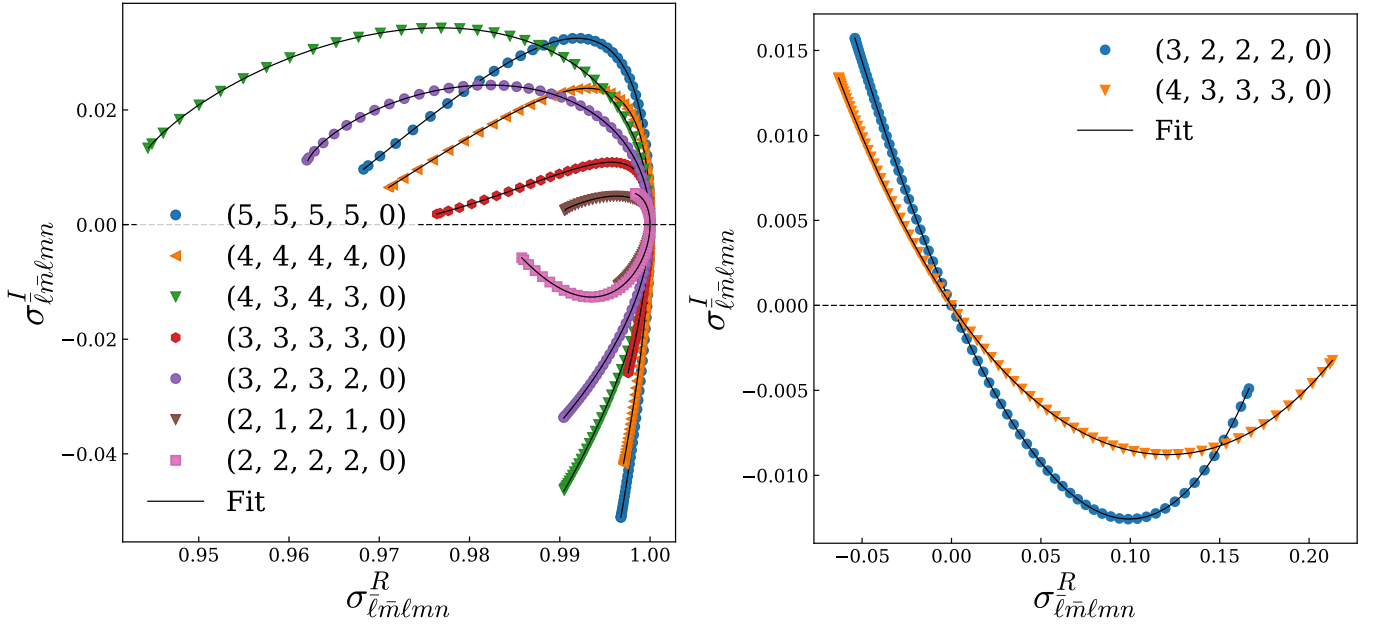


FIG. 2. Spherical-spheroidal harmonic mixing coefficients.